Hellsten, Niko; Karttunen, Antti; Engblom, Charlotta; Reznichenko, Alexander ; Rantala, Erika

Compressive Properties of Micro-spherical SiO2 Particles

Published in:
Advances in Powder and Ceramic Materials Science

DOI:
10.1007/978-3-030-36552-3

Published: 01/01/2020

Document Version
Peer reviewed version

Compressive properties of micro-spherical SiO_2 particles

Niko Hellstén[1+], Antti J. Karttunen[1], Charlotta Engblom,[2] Alexander Reznichenko[2+], Erika Rantala[2]

[1]Aalto University, School of Chemical Engineering, P.O. Box 16100 Aalto, Finland, email: firstname.lastname@aalto.fi

[2]Borealis Polymers Oy, PL 330 06101 Porvoo, Finland

[+]email of corresponding author: niko.hellsten@aalto.fi

[+]alexander.reznichenko@borealisgroup.com

Keywords: Micro-compression, micro-spherical silica, catalysts

Abstract

Micron-sized, spherical SiO_2 particles are important various industrial applications, such as in heterogeneous catalyst preparation. In particular, many of industrially relevant olefin polymerization catalysts are currently prepared using micro-spherical silica as catalyst support. In large-scale catalytic polyolefin production, the quality of the final product, as well as the process efficiency is crucially dependent on overall consistency, quality, physico-chemical properties of the catalyst. As the catalyst particle experiences various stresses during the polymer particle growth, mechanical properties of catalyst play a key role in its performance in the polymerization process. However, there is currently a lack of experimental mechanical property measurements of micron-sized, spherical SiO_2 particles relevant for the polyolefin catalyst production.

In this work, compressive properties of commercial porous micro-spherical silicas were studied using a quasi-static micro-compression method. The method includes compressing single, micron-sized particles in controlled loading conditions. From the measurements, the compressive elastic-plastic properties of these particles can be determined.

Introduction

Mechanical properties of solid catalyst materials are important in many industrial processes [1, 2]. In polyolefin production, the particle strength and structural integrity of heterogeneous Ziegler-Natta (ZN), Phillips, metallocene or late transition metal catalysts directly affects the quality of polymer produced, in particular affecting fragmentation and generation of undesired polymer fines in the polymerization process [3, 4]. The commonly used heterogeneous ZN catalysts are porous spheres or quasi-spheres of 10–100 μm in diameter, and comprise a transition metal component, organometallic co-catalyst and are produced using $MgCl_2$ or SiO_2 support. Consequently, experimentally measured mechanical strength data of the respective catalyst support materials, such as micro-spherical, porous SiO_2 particles can provide an important insight for selecting adequate catalyst support for process optimization [1].

Strength of materials depends on their density, porosity and microstructure (crystallinity, flaws, flaw distribution) and dictates their responses to external mechanical forces [5]. These responses include deformation and fracture characteristics under uniaxial or multiaxial stresses. Based on their strain behavior and fracture type, materials are either brittle or ductile. Ceramic materials, such as Al_2O_3 and SiO_2, are generally brittle and exhibit mainly elastic deformation prior to fracture [6].

Spherical shape of catalyst particles limits the study of their mechanical properties. Thus, compression tests ('Crushing' tests) and impact tests, rather than tensile tests, have been used to study strengths of spherical catalyst carrier materials, both in macro- (>1 mm) and micron-size (<1 mm) [2, 7]. These previous studies confirm the brittle nature of Al_2O_3 and SiO_2 and reveal a scatter in the measured breaking loads and strengths.

This scatter is due to initiation of failure in a randomly distributed flaw, possibly with less force than the material strength. Consequently, measurement of the intrinsic material strength is difficult, and statistical methods such as Weibull distribution analysis are applied to better estimate material failure.

While experimental measurements of the strength of silica exist, experimental data is still lacking for porous micro-spherical silica. In this work, the compressive properties of micro-spherical, porous 16.5 – 49.4 µm diameter silica particles were studied experimentally using the micro-compression method. This method is similar to the American Society for Testing and Materials (ASTM) compression test for samples with dimensions greater than 1 mm [8]. From the measurements, the breaking strengths of single particles were calculated.

Materials and methods

Table I shows properties of the tested porous, micro-spherical materials. Due to assumed sample brittleness, a minimum of 40 measurements of each sample were conducted to increase statistical reliability of the results. True densities of the samples were determined via He gas pycnometry method, using [9] AccuPyc 1330 instrument from Micromeritics.

Table I. Properties of the tested silicas.

Sample	# of individual particle measurements	Diameter range (µm)	Average size (µm)
A	40	23.4–49.4	34.9
B	42	16.5–45.9	28.3

All of the micro-compression measurements were conducted using a Shimazdu MCT-511 micro compression tester. Figure 1 depicts a schematic of the setup. It consists of a computer-controlled stage, upon which the lower compression plate is fastened, optical microscope for sample positioning and force controlled upper compression head. The displacement and force measurement sensors are located at the upper part of the tester in close contact with the upper compression head.

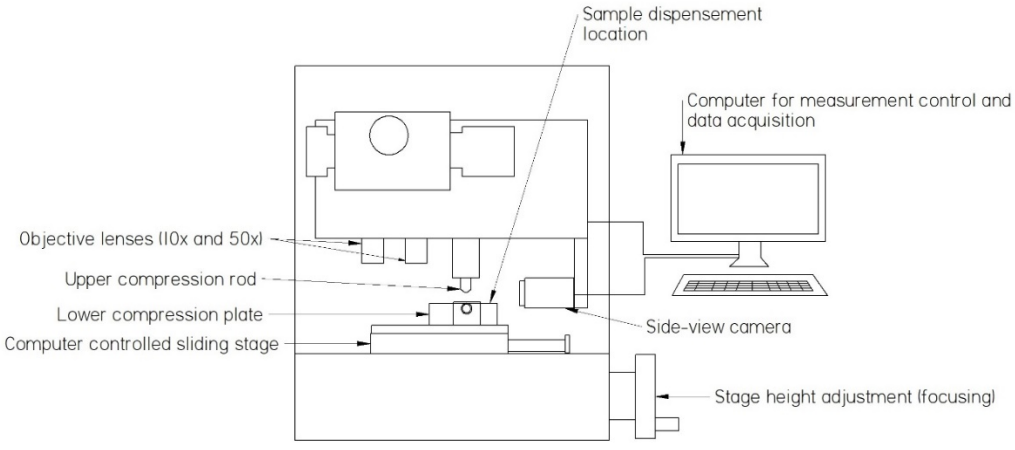

Figure 1. Schematic of the micro-compression setup.

Table II shows the conditions of the micro-compression measurements.

Table II. Conditions of the micro-compression measurements.

Indenter type	Flat indenter with a 50 µm diameter diamond tip
Objective lens for size measurement	50x
Measure mode	Single
Test mode	Compression
Test form	Particle
Test end condition	Breaking point
Test force (mN)	20
Loading rate (0.4462 mN/sec)	10.0
Holding time at load (sec)	5
Compression ratio	10%

As the particle sizes ranged from 16.5 to 64.3 µm, a 50 µm diameter flat tip diamond indenter was used. In the beginning of a measurement set, the surface of the lower compression plate was cleansed with alcohol, dried and fastened to place. Next, the sample particles were dispensed onto it using microspatulas. Typically, in one dispensing several particles ended on the lower compression plate (Figure 2-a). When the sample was in place, the measurement parameters were set using the control and analysis software provided with the device. For the measurements reported here, the compression mode was used. In this mode, the sample is compressed with a fixed loading rate until the set test force value is reached, and then held for a set time after which the test ends by the compression head returning to its original position. Other test modes for this equipment are cyclic and load-unload. For these measurements, the sample breakage was chosen as the end condition. This means that if the particle breaks before reaching maximum force, the measurement ends.

Test force of 20 mN and slow loading rate of 0.4462 mN/sec were chosen based on initial test measurements at higher forces and faster rates, which resulted in particles flying away from the lower compression plate. Suitably isolated single particles for the measurement were located using the optical microscope and computer-controlled motorized stage of the micro-compression tester. A specimen suitable for testing must be located far enough from any other particles so that only the selected particle is compressed during measurement. In case where all particles were located too close to each other, they were dispersed using a small blow of compressed air. When a suitable particle was found, its diameter was measured via digital image analysis, taking the image using 50x objective lens in the optical microscope focused onto the equatorial level of the sample. After sample size measurement, the microscope was focused on top of the sample to prevent the compression head from hitting the samples or stage, the stage was moved from the observation side to the indentation side and compression initiated. Monitoring the sample position during compression measurement is possible from one direction using the side-view camera included in the device.

In the compression measurement, the compression head is lowered until it detects the sample surface. Then the compression force increases according to the set rate. The sample surface is detected from the increase in resistance confronted by the compression head. The breaking force of each sample, displacement of the compression head from the surface, breaking and reference strengths are reported. Displacement and force are directly measured while breaking and reference strengths are calculated according to equation 1. The reference strength is the calculated pressure required to deform the sample to a set value of its original size. In the measurements reported here, this value was set to 10%.

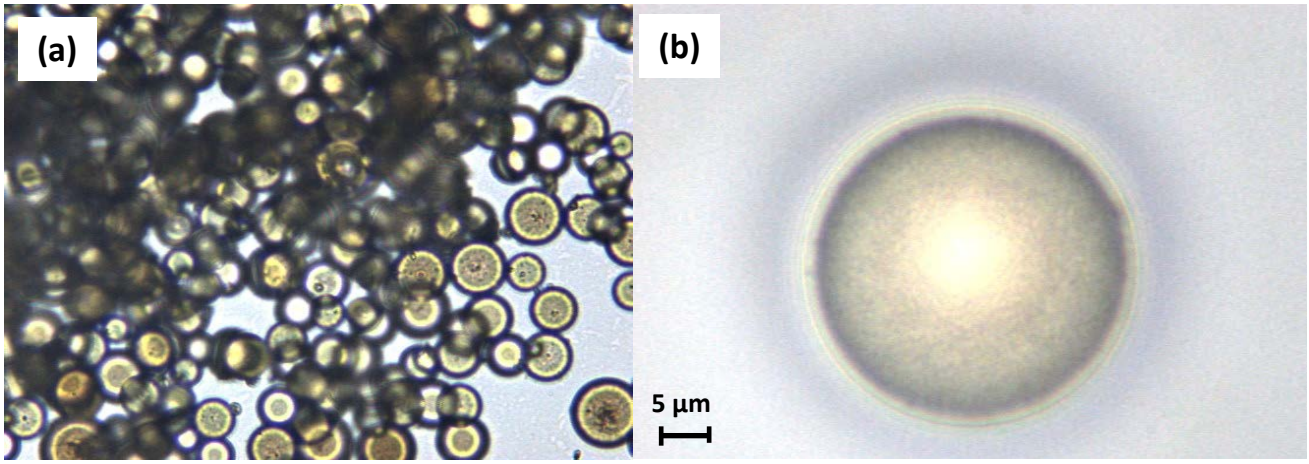

Figure 2. (a) Multiple particles too close to each other and (b) a particle focused for size measurement and compression.

Results and Discussion

In this study, two types of commercially available porous micro-spherical silicas were investigated by uniaxial quasi-static micro-compression method. The crushing strengths of 40 particles of silica type A and 42 particles of silica type B were investigated by uniaxial quasi-static micro-compression method. The number of particles tested was selected in order to achieve statistically significant results (Table I). Each tested particle broke during the compression sequence. Table III shows the breaking load, breaking stress and stress at 10% deformation of the measurements. True densities of the sample A and B were 2.25 and 2.26 g/cm^3, respectively as measured by gas pycnometry.

Table III. Statistical values of the compressed SiO_2 samples.

Sample	A	B
Load (mN)		
Mean	5.04	1.80
Median	4.84	1.63
Standard deviation	1.49	0.74
Range of values	1.85 – 8.71	0.33 – 4.08
Breaking stress (MPa)		
Mean	3.30	1.81
Median	3.33	1.88
Standard deviation	0.85	0.53
Range of values	1.79 – 6.45	0.27 – 2.83
Stress at 10% (MPa)		
Mean	1.72	1.53
Median	1.70	1.64
Standard deviation	0.70	0.61
Range of values	0.31 – 4.47	0.27 – 2.58

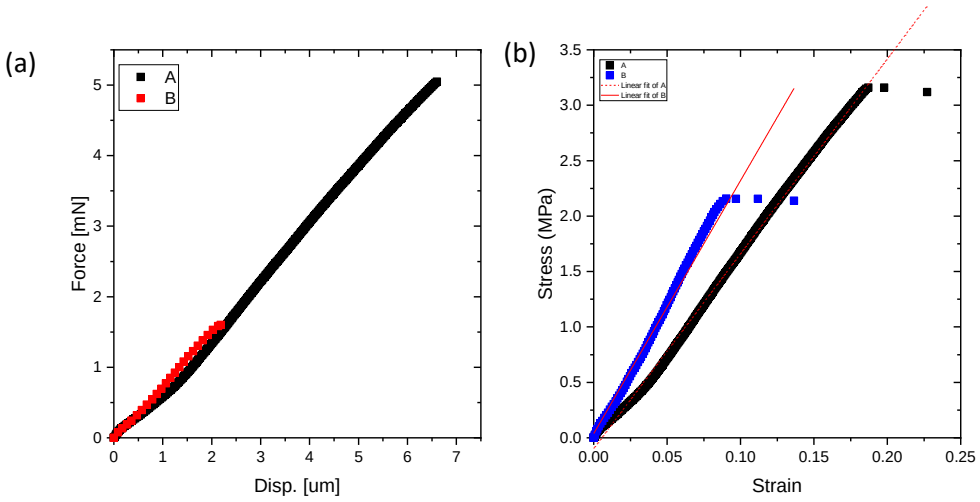

Figure 3. Typical force-displacement (a) and stress-strain (b) curves for the studied samples.

During testing, the force and displacement values are directly measured. Nevertheless, as the breaking force and displacement (deformation) are size-dependent, the more conventional stress-strain curves have been calculated using equations 1 and 2, respectively. Figure 3 shows typical force-displacement and stress-strain curves of the two samples. Equation 1 was introduced by Hiramatsu and Oka [10] to calculate the ultimate strength of spherical samples in compression. Equation 2 is the conventional calculation of linear strain. In this case, only the linear strain along the compression axis, e.g. the flattening of the sample, is considered (Figure 5).

$$\sigma = 2.8 \cdot \frac{P}{\pi d^2} \quad (1)$$

$$\varepsilon = \frac{Measured\ deformation}{Original\ diameter\ of\ sphere} \quad (2)$$

In equations 1 and 2, σ is the breaking strength (MPa), P the measured breaking force (N), d the diameter of the sample (mm) and ε the axial strain. Typically, a negative sign is used for compression measurements as the length of a sample actually decreases. In this work, it was decided to use positive values for strain for easier interpretation of the curves.

Figure 3 shows that both samples exhibit typical brittle material behavior. The curves are almost straight lines until the point of breakage, indicating mainly an elastic deformation. For both samples, there is a small change in the angle of the curve at 0.03 strain for the silica A and 0.02 strain for silica B. After these points, the curve gets steeper. This angle can indicate a yield point of the sample or small internal breakage and elastic deformation before the sample enters the elastic-plastic region [2, 11]. The variance in the relative axial deformations in these experiments was large, ranging from 7.13% to 67.70%.

The mean values indicate that, the silica type A is stronger towards crushing in comparison to type B. The median values of the measurements for both samples are close to the mean values suggesting that the mean is a good measure of the measured samples. Nevertheless, the range of measured breaking force and calculated strength values are larger than the mean values indicating considerable scatter. Figure 4 represents the arrangement in compression measurement with contact points between the upper flat indenter and sample marked with A, and contact point between the sample and lower compression plate marked with B. The small

circles represent the randomly distributed flaws. As particle failure can initiate in any of the flaws and with a lesser stress than the intrinsic material strength would require, a scatter in compressive strength measurements for brittle materials is typical. While the classical theories state that strength of a material is constant throughout its volume, experimental measurement of this is extremely difficult. Nevertheless, variable results can be due to anisotropy of a material. In addition, sample volume affects strength properties and the size of the tested sample should always be reported. Due to the inability of the classical theories of strength to explain the scatter, the statistical theory of Weibull [12] is often applied in predicting probability of failure under a specified stress.

The two-parameter Weibull distribution equation is

$$F(\sigma) = 1 - \exp(-\beta_0 \sigma^m) \quad (3)$$

Where $F(\sigma)$ is the probability of failure, σ the maximum stress within the sample, β_0 a size parameter and m the Weibull modulus. The Weibull parameters can be obtained by first reorganizing equation 5 and taking natural logarithms from both sides to give

$$lnln(\frac{1}{1-F(\sigma_i)}) = mln\sigma + ln\beta_0 \quad (4)$$

To obtain the probability of failure for each particle, the strength failure data of each tested particle is organized in ascending order and ranked accordingly. An estimated cumulative probability of failure is then given by:

$$F(\sigma_i) = \frac{i-0.5}{N} \quad (5)$$

The probability of failure and failure strength of each tested particle are used to obtain the Weibull parameters β_0 and m by linear regression. This approach was adopted from Subero-Couroyer et al. [13]. Figure 5 shows the Weibull probability and the survival plots for the tested materials. The Weibull probability plot shows how well a set of data follows the Weibull distribution. In contrast, the Weibull survival plot describes probability of particle failure under a specific stress.

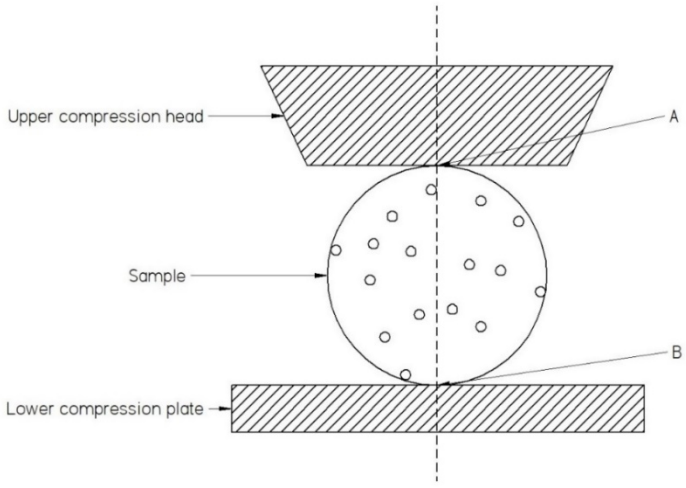

Figure 4. Schematic of particle compression between two flat plates. A and B mark the initial contact points while the dashed line denotes the compression axis. The small circles represent randomly distributed flaws.

Figure 5 shows that silica A has a higher probability to survive at greater stresses than B. In contrast, silica B results (R^2 = 0.93) fit better to the Weibull distribution in comparison to the results from type A (R^2 = 0.90). The Weibull modulus and σ_0 for A are higher than for B suggesting a stronger, more homogeneous material.

Table IV. Parameters obtained from Weibull analysis.

Weibull analysis	A	B
Weibull modulus, m	4.9	3.0
β_0	$1.87 \cdot 10^{-3}$	0.12
Scale parameter, σ_0 (MPa)	3.6	2.1
R^2	0.903	0.928

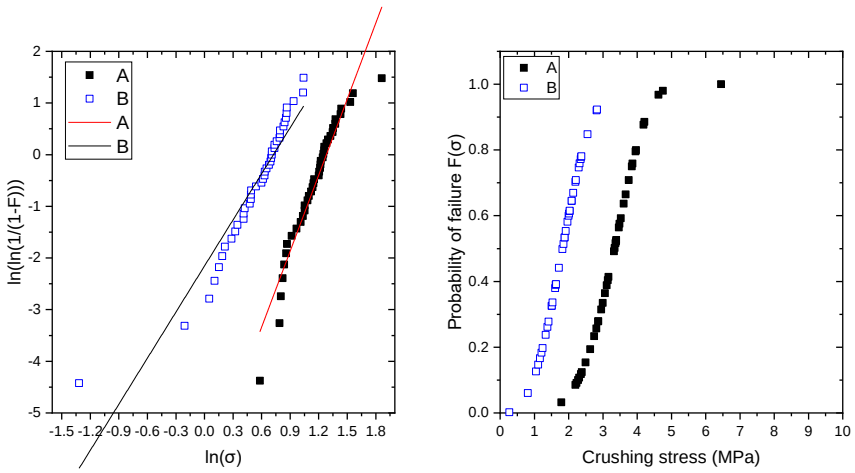

Figure 5. Weibull probability (a) and survival (b) plot.

Comparing the results of this work with previous compression measurements of micro-spherical SiO_2 shows that the breaking strengths obtained in this work are two orders of magnitude smaller than those measured previously for fused amorphous SiO_2. Porosity may explain these differences as in comparison, Ryshkewitch [14] found that increasing porosity in Al_2O_3 can decrease its strength by two orders of magnitude from ~1000 MPa to 10–20 MPa .

Table V. Previously measured experimental data for microspherical SiO_2.

Sample	Diameter (μm)	Breaking strength (MPa)	Yield strength (GPa)	Young's modulus (GPa)	Ref
Fused amorphous	20-60	900			[2]
Sicastar plain (amorphous)	0.5		6.1	44.7	[15]
Amorphous	0.5-0.8			30.8	[16]
TYPE B	16.5-45.9	1.81			This work
TYPE A	23.4-49.4	3.30			This work

Conclusions

In this work, micro-compression method was successfully used to measure breaking strengths of two different types of microporous SiO_2 particles. For statistical reliability, 40 and 42 individual particles of the materials were measured, respectively. Both materials exhibited brittle fracture behavior and large scatter in the results, as expected. Statistical Weibull method was applied to the results to estimate breaking probabilities of the

materials. Silica A was found to be mechanically stronger than silica grade B. Based on the Weibull analysis, 92% of silica B fail at 2.8 MPa compressive stress while 100% of A fail at 6.5 MPa compressive stress. As the true densities of the samples measured by gas pycnometry are similar, these differences are likely to originate from the morphological differences such as porosity, pore connectivity and pore size distribution. In addition, differences between previous studies of micro-spherical fused amorphous SiO_2 and this work suggest a strong effect on compressive strength due to porosity and further studies are required to confirm this.

References

[1] D. Wu, J. Zhou, Y. Li, Mechanical strength of solid catalysts: Recent developments and future prospects, AIChE J. 53 (2007) 2618-2629.

[2] V. Pejchal, G. Žagar, R. Charvet, C. Dénéréaz, A. Mortensen, Compression testing spherical particles for strength: Theory of the meridian crack test and implementation for microscopic fused quartz, J. Mech. Phys. Solids. 99 (2017)70-92.

[3] J.B.P. Soares, T.F. McKenna, Polyolefin reaction engineering, Wiley-VCH ; John Wiley [distributor], Weinheim : Chichester, 2012.

[4] R. Hoff, R.T. Mathers (Eds.), Handbook of Transition Metal Polymerization Catalysts, John Wiley & Sons, Incorporated, Hoboken, 2010.

[5] W.F. Hosford, Mechanical Behavior of Materials, Cambridge University Press, New York, 2009.

[6] J. Pelleg, Mechanical properties of ceramics, Springer, Cham, 2014.

[7] C. Couroyer, Z. Ning, M. Ghadiri, N. Brunard, F. Kolenda, D. Bortzmeyer, P. Laval, Breakage of macroporous alumina beads under compressive loading: Simulation and experimental validation, Powder Technol. 105 (1999)57-65.

[8] K.J. Hemker, W.N. Sharpe, Microscale characterization of mechanical properties, Annu.Rev.Mater.Res. 37 (2007) 93-126.

[9] A.A. S Tamari and, Optimum design of the variable-volume gas pycnometer for determining the volume of solid particles, Meas. Sci. Technol. 15 (2004) 1146.

[10] Y. Hiramatsu, Y. Oka, Determination of the tensile strength of rock by a compression test of an irregular test piece, Int. J. Rock Mech. Min. Sci. Geomech. Abstr. 3 (1966)89-90.

[11] M. Khanal, W. Schubert, J. Tomas, Compression and impact loading experiments of high strength spherical composites, Int. J. Miner. Process. 86 (2008)104-113.

[12] W. Weibull, A statistical theory of the strength of materials, Ingenioersvetenskapsakad., Handl. No. 151 (1939) 45 pp.

[13] C. Subero-Couroyer, M. Ghadiri, N. Brunard, F. Kolenda, Weibull analysis of quasi-static crushing strength of catalyst particles, Chem. Eng. Res. Des. 81 (2003)953-962.

[14] E. Ryshkewitch, Compression strength of porous sintered alumina and zirconia, J Am Ceram Soc. 36 (1953) 65-68.

[15] S. Romeis, J. Paul, M. Ziener, W. Peukert, A novel apparatus for in situ compression of submicron structures and particles in a high resolution SEM, Rev.Sci.Instrum. 83 (2012) 095105.

[16] J. Paul, S. Romeis, J. Tomas, W. Peukert, A review of models for single particle compression and their application to silica microspheres, Adv. Powder Technol. 25 (2014)136-153.